JAAS

Accepted Manuscript

This is an *Accepted Manuscript*, which has been through the Royal Society of Chemistry peer review process and has been accepted for publication.

Accepted Manuscripts are published online shortly after acceptance, before technical editing, formatting and proof reading. Using this free service, authors can make their results available to the community, in citable form, before we publish the edited article. We will replace this *Accepted Manuscript* with the edited and formatted *Advance Article* as soon as it is available.

You can find more information about *Accepted Manuscripts* in the Information for Authors.

Please note that technical editing may introduce minor changes to the text and/or graphics, which may alter content. The journal's standard Terms & Conditions and the Ethical guidelines still apply. In no event shall the Royal Society of Chemistry be held responsible for any errors or omissions in this *Accepted Manuscript* or any consequences arising from the use of any information it contains.

ROYAL SOCIETY OF CHEMISTRY

www.rsc.org/jaas

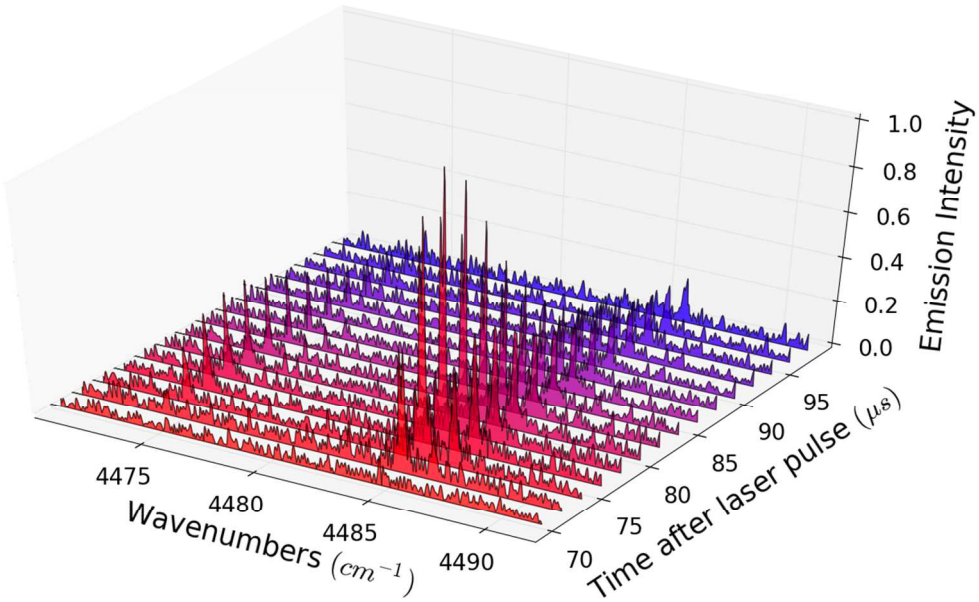

The synchronous continuous scanning method is used for the measurement of the time resolved Fourier-transform infrared LIBS of atomic Indium.
439x273mm (72 x 72 DPI)

Laser ablation of indium target: time-resolved Fourier-transform infrared spectra of In I in the 700–7700 cm^{-1} range

S. Civiš,*[a] P. Kubelík,[a,c] M. Ferus,[a] V. E. Chernov,[b] E. M. Zanozina,[a,c] and L. Juha[c]

Received Xth XXXXXXXXXX 20XX, Accepted Xth XXXXXXXXX 20XX
First published on the web Xth XXXXXXXXXX 200X
DOI: 10.1039/b000000x

Laser-induced breakdown spectroscopy (LIBS) in combination with time-resolved Fourier-transform technique was applied to obtain spectra of In I in the infrared spectral region. This method was proven to be suitable for measuring the weak energy transitions between highly excited Rydberg atomic levels. The advantage comes from the possibility of selecting an optimal time-delay after the laser pulse, when the low intensity spectral lines are near their maximum intensity and can filter out the disturbing high intensity lines with different emission time profiles. The time-resolved spectra were recorded in the 700–1000, 900–1300, 1200–1680, 1800–4000, 4100–5000 and 5000–7700 cm^{-1} ranges with a resolution of 0.017 cm^{-1}. Using this technique, we obtained five *g*- and *h*-levels of In I that have never been measured previously. We demonstrate a close similarity of wavenumbers for the $7s_{\frac{1}{2}}$–$7p_{\frac{1}{2}}$ and $4f$–$5g$ transitions of the In atom.

1 Introduction

Following a recent experiment [1] on laser trapping and cooling of the In atom, it was proposed [2] that this atom could be considered a possible candidate for searching for the permanent electric-dipole moment. In view of this proposition, several important spectroscopic characteristics, such as hyperfine constants, [3] one-electron transition probabilities [4] and Stark shifts, have been recently measured [5] and calculated. [6] However, despite more than a century of spectroscopic studies, [7,8] not all of the In Rydberg states are known.

Similar to the other elements of the third group, all of the electronic states of In I are subdivided into two configuration systems, which can be considered as excitations of one or more electrons from the ground-state configuration $5s^2 5p$. The first system consists of the doublet $5s^2 nl\ ^2L_J$ terms, whose total orbital, L, and angular, $J = L \pm \frac{1}{2}$, momenta are determined by the orbital momentum $l = L$ of the single excited *nl*-electron over the closed $5s^2$ core. For brevity, these terms are henceforth denoted as nl_J. The other three-electron configuration system $5snln'l'$ is due to an excitation of two electrons, including one from the 5*s* core. These configurations give rise to the ^4P, ^2S, ^2P and ^2D terms in the *LS* coupling scheme (see Connerade and Baig [9] for the intermediate coupling assignment), from which only the quadruplet $5s5p^2\ ^4P_{1/2,3/2,5/2}$ terms [10] lie below the first ionization threshold, while the doublet $5s5p^2\ ^2S_{1/2}$, $5s5p^2\ ^2P_{1/2,3/2}$, [11–13] and $5s5pnp\ ^2P_{3/2}$ ($n = 6,7,8$) [14] terms are autoionizing states excited above the threshold. Higher excited series of doubly excited In states were studied assuming more a complex J_cK coupling scheme $5s5p^{S_c}\ ^3P_{J_c}np$ with $S_c = 3$, $J_c = 0,1$ (n = 6–9, [15] n = 6–26 [16]), $J_c = 2$ (n = 6–9 for $S_c = 3$ and n = 6–13 for $S_c = 1$) [16] and $S_c = 3$, $J_c = 1$ (n = 16–31). [17] A strong configuration interaction due to these two-electron excitations influences the other states' spectral parameters, such as the quantum defect of the Rydberg states, fine- and hyperfine-structure splitting, and transition amplitudes. [13]

The energies of the In $5s^2nl$ states with $l \leq 3$ and $n < 10$ were measured by Johansson and Litzén [18] and George *et al.* [19] during discharge. A higher excited (Rydberg) *nl* was first obtained from a UV absorption spectra in a furnace by Garton and Codling [20] (*ns* (n = 9–29), $np_{1/2}$ (n = 14–23), $nd_{3/2}$ (n = 8–19) and $nd_{5/2}$ (n = 8–34) series) and then by Penkin and Shabanova [21] (*ns* (n = 23–30) and $nd_{3/2,5/2}$ (n = 31–39) series). Some years later, the Rydberg *nl* states of In were studied using two-photon laser spectroscopy. The energies of the highly excited $np_{3/2}$ (n = 11–42), $np_{1/2}$ (n = 11–13) and $nf_{5/2}$ (n = 8–31) states of In were measured by Mirza and Duley [22]. A few years later, Neijzen and Dönszelmann extended these measurements with a higher level of precision using a pulsed dye laser. They measured the energies the of highly excited $ns_{1/2}$ (n = 26–80), $nd_{3/2}$ (n = 25–70), $nd_{5/2}$ (n = 25–80) [23] and $np_{1/2,3/2}$ (n =

† Electronic Supplementary Information (ESI) available: [details of any supplementary information available should be included here]. See DOI: 10.1039/b000000x/

[a] *J. Heyrovský Institute of Physical Chemistry, Academy of Sciences of the Czech Republic, Dolejškova 3, 18223 Prague 8, Czech Republic. Fax: +420 28658 2307; E-mail: civis@jh-inst.cas.cz*
[b] *Voronezh State University, 394693 Voronezh, Russia.*
[c] *Institute of Physics, Academy of Sciences of the Czech Republic, Na Slovance 2, 18221 Prague 8, Czech Republic.*

24–54)[24,25] states as well as the fine structure splittings of the np (n = 17–29,[26] n = 24–54[25]) and nd (n = 17–31[26], n = 25–70[25]) levels. The fine structure splitting of the Rydberg $5s^2np\ ^2P_{1/2,3/2}$ states (n = 27–35) and the isotopic shift of the two-photon transitions in ^{113,115}In were measured using a thermionic diode.[27] The most recent measurement of the first In ionization potential was performed by Kasimov *et al.*[28], who measured the Rydberg $np_{1/2,3/2}$ (n = 12–60) and $nd_{3/2,5/2}$ (n = 15–30) series using two-step laser excitation and ionization.

However, no In I states with $l > 3$ (*e.g.*, *g*- or *h*-levels) have been observed. According to simple estimates with the help of the Rydberg formula,[29] *e.g.*, the $5s\,5g$-$5s\,6h$ transitions should appear in the infrared (IR) region with wavenumbers near $\nu \simeq 1300$ cm^{-1}, $5s\,6g$-$5s\,7h$ and transitions near $\nu \simeq 800$ cm^{-1}. The transitions involving higher l-states can be observed in an even longer wavelength spectral range. To the authors' knowledge, there are only two IR measurements of In I spectra available: Johansson and Litzén[18] ($\nu > 4180$ cm^{-1}) and George *et al.*[19] (ν = 2559–11518 cm^{-1}); therefore, new IR measurements are needed to access the high-l states.

The IR region plays an increasingly important role in modern astronomy, *e.g.*, in studies of cool stars, planets, dust clouds etc. The powerful capacity of IR astronomy cannot be fully utilized without detailed spectroscopic information on the atomic line features (in particular, wavelengths and oscillator strengths) in the IR region.[30] The aim of the present study is to observe In I lines in the IR domain, including the 800–2500 cm^{-1} range where no In I spectra have been recorded previously. We extend the knowledge regarding the spectrum of the neutral indium atom by reporting the energies of some its high l (*g*- and *h*-) states and also provide the calculated probabilities and oscillator strengths for the transitions in the measured spectral domain.

2 Experimental methods

Time-resolved FTIR spectrometry

This work continues the series of Fourier transform infrared (FTIR) spectroscopic studies of metal atom IR spectra.[30–38] The time-resolved FTIR spectroscopy is an experimental technique that was originally developed and used for studying the kinetics of various physical and/or chemical[39] processes occurring in dynamic systems.

FT spectroscopy has several advantages over the usual diffraction methods.[40] For our applications, the ability to obtain spectra over a wide wavenumber range (in comparison with,*e.g.*, the laser spectroscopy[41]) and with a high spectral resolution are the most important characteristics.These main features allowed us to explore a wide portion of the spectrum in the infrared region and enabled the effective search for new spectral transitions that have not previously been observed.

In the present work, the synchronous scanning FT technique is used.[42] This time-resolved method requires the transient phenomena (laser ablation of the metal target) to be induced periodically and synchronously by using He-Ne laser (the internal wavenumber standard of the FT spectrometer) fringe signals. The triggers based on the He-Ne laser fringes are used also for the data sampling. The time synchronization of the sample ablation and the data acquisition is controlled by a FPGA processor programmed by QUARTUS II 7.1, Altera.

This experiment was carried out in combination with a pulse laser whose maximum repetition rate is slower than the He-Ne fringe frequency. In this case, there is no possibility of sampling at each individual trigger point of the He-Ne laser. To overcome this instrumental limitation, the 1/n sampling method is used.[43] The laser ablation is triggered at every *nth* He-Ne fringe. This undersampling condition requires n scans (interferometer mirror movements) to assemble a complete interferogram. The timing diagram for the interleaved sampling is shown in Figure 1.

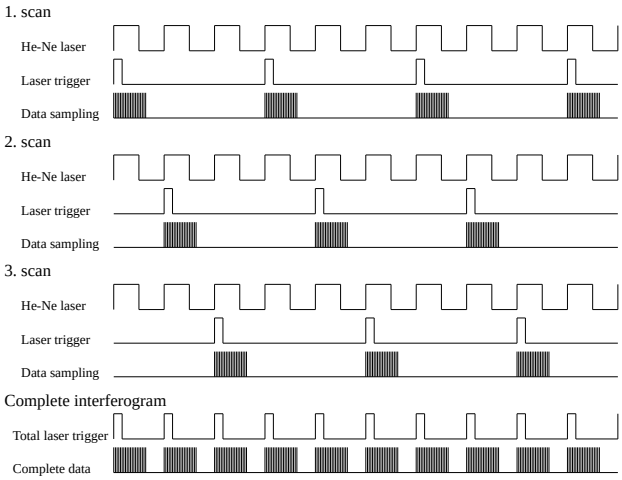

Fig. 1 The timing diagram for the $1/n$ interleaved sampling ($n = 3$)

Sample preparation

The vapors of the excited In atoms are produced during the ablation of the metal indium target (with a natural isotopic composition) by a high-repetition rate (1.0 kHz) pulsed nanosecond ArF laser (ExciStar S-Industrial V2.0 1000, with a pulse length of 12 ns, $\lambda = 193$ nm, output energy of 15 mJ, and fluency of approximately 2–20 J/cm^2) inside a vacuum chamber (average pressure 10^{-2} Torr). The vacuum chamber scheme is shown in Figure 2.

Emission spectra registration

The infrared emission was focused into the spectrometer using

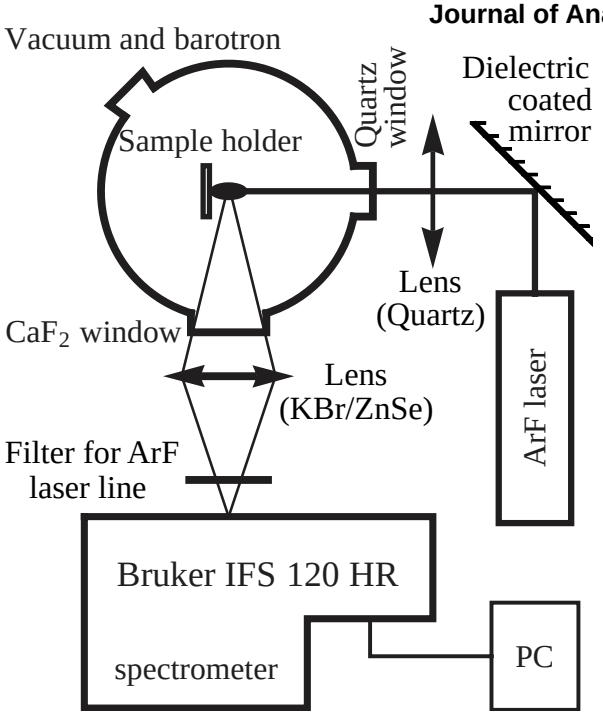

Fig. 2 Setup of the LIBS experiment

a CaF_2 or ZnSe lens (for 2000–7700 cm^{-1} or 700–2000 cm^{-1}, respectively). The time-resolved FTIR spectra were measured using a modified Bruker IFS 120 HR spectrometer. KBr/CaF_2 optics and HgCdTe (MCT)/InSb detectors were used for the 700–2000 cm^{-1} and 2000–7700 cm^{-1} ranges, respectively. During a single measurement, 30 time-resolved interferograms were registered with a maximum time resolution of 1 μs and spectral resolution of 0.0017 cm^{-1}.

In the emission measurement mode, the registration of relatively low intensity spectral lines can be disturbed by the strong lines occurring in the spectrum near the measured low intensity lines. The application of the time-resolved measurement made it possible to choose an optimal time-delay after the laser pulse when the weak spectral lines are near their maximum intensity. This method also filters out the disturbing high intensity lines with different emission time profiles. Figure 3 shows an example of when the emission intensities of the spectra have a complex dependence on the time delay τ after the ArF laser pulse shot. The analysis of these atomic emission time-profiles in our LIBS experiment confirms the complexity due to the non-equilibrium and non-stationary conditions of the plasma for the excited states. [44]

Therefore, the use of the time-resolved scheme is essential in our experiment. This method has allowed us to measure the weak spectral transitions that have not been previously observed.

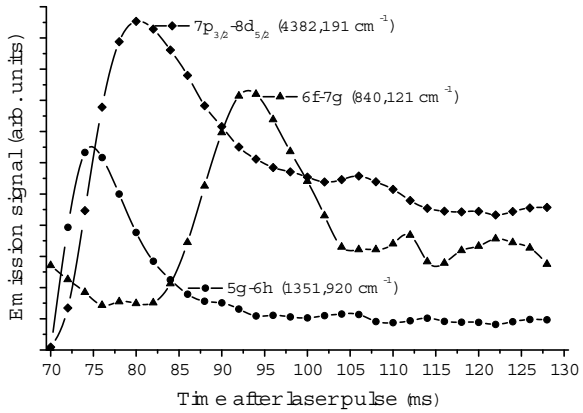

Fig. 3 Time profiles of several In emission lines

3 Results and Discussion

Table 1 reports the measured line features: wavenumbers, widths and intensities, which were derived from fitting to a Lorentzian line shape. The measurements were performed in six spectral ranges: 700–1000, 900–1300, 1200–1680, 1800–4000, 4100–5000 and 5000–7700 cm^{-1}. Only lines within the same spectral range have intensities with the same scale. For all numerical values, their uncertainties are reported in parentheses immediately following the values. They should be treated as the rightmost significant digits, *e. g.*, 123.4(56) means 123.4 ± 5.6.

Some wavenumbers reported in other studies of In I IR spectra [18,19] are given in Table 1 for comparison. Our wavenumbers are consistent with previous results, [18,19] when available, within the uncertainty range. George *et al.* [19] reported very precise (error < 0.005 cm^{-1}) measurements of indium iodide FT spectra in a microwave-excited discharge tube, where the hyperfine structure for ten lines was resolved. For some of these lines, Table 1 lists the centers of gravity of their hyperfine patterns. The accuracy of the measurements by Johansson and Litzén [18] is greater than 0.02 cm^{-1}. The error estimation of the results of the present work was described recently. [37,38]

As mentioned above, no values for the In I *ng* and *nh* energy levels are available in the literature. To identify the lines corresponding to these levels, we first calculated the approximate energies of these states using the Rydberg formula. In the case of transitions with close wavenumbers, we compared the theoretical intensities of such emission lines that are, in turn, dependent on the oscillator strengths of the corresponding transitions. The oscillator strengths (f-values) were calculated using single-channel quantum defect theory (QDT).

[a] *the center of gravity of the hyperfine pattern*

Table 1 Observed In I line wavenumbers ν_{ki}, intensities I_{ki}, signal-to-noise ratios (SNR), full widths at half-maxima (FWHMs)

Line wavenumbers ν_{ki} (cm^{-1})			I_{ki}	SNR	FWHM	Identification
Present work	George *et al.* [19]	Johansson and Litzén [18]	(arb. u.)		(cm^{-1})	
815.430(8)			1.85×10^4	6.7	0.069(31)	$6g$–$7h$
840.121(29)			1.57×10^4	2.37	0.129(104)	$6f$–$7g$
1190.154(5)			7.53×10^3	10.	0.069(18)	$8s_{\frac{1}{2}}$–$8p_{\frac{1}{2}}$
1244.442(4)			1.33×10^4	16.	0.066(12)	$8s_{\frac{1}{2}}$–$8p_{\frac{3}{2}}$
1351.920(3)			3.41×10^4	32.	0.088(9)	$5g$–$6h$
1392.953(4)			1.18×10^4	20.	0.098(11)	$5f$–$6g$
2128.818(6)			1.05×10^3	10.	0.078(16)	$4f_{\frac{5}{2}}$–$7d_{\frac{3}{2}}$
2154.402(8)			1.73×10^3	9.1	0.144(24)	$4f_{\frac{7}{2}}$–$7d_{\frac{5}{2}}$
2161.471(4)			2.50×10^3	1.5	0.096(12)	$5g$–$7h$
2204.538(4)			2.77×10^3	9.2	0.123(14)	$5f$–$7g$
2544.276(11)			1.47×10^3	7.5	0.144(33)	$7d_{\frac{5}{2}}$–$7f_{\frac{7}{2}}$
2559.586(8)	2559.584[a]		1.87×10^6	9.8	0.077(12)	$7s_{\frac{1}{2}}$–$7p_{\frac{1}{2}}$ / $4f$–$5g$
2559.638(1)			1.39×10^6	15.	0.037(3)	
2569.860(6)			9.53×10^2	10.	0.070(18)	$7d_{\frac{3}{2}}$–$7f_{\frac{5}{2}}$
2671.005(1)	2671.047[a]		4.43×10^5	9.7	0.057(3)	$7s_{\frac{1}{2}}$–$7p_{\frac{3}{2}}$
2671.090(2)			2.70×10^5	8.6	0.038(7)	
2778.576(5)			1.57×10^3	15.	0.104(15)	$6d_{\frac{3}{2}}$–$8p_{\frac{1}{2}}$
2783.016(10)			2.29×10^3	10.	0.191(32)	$6d_{\frac{5}{2}}$–$8p_{\frac{3}{2}}$
2863.525(3)	2863.510		4.45×10^3	20.	0.120(10)	$7p_{\frac{3}{2}}$–$7d_{\frac{3}{2}}$
2889.066(2)	2889.067		4.26×10^4	22.	0.160(5)	$7p_{\frac{3}{2}}$–$7d_{\frac{5}{2}}$
2974.996(2)	2974.995		2.14×10^4	25.	0.137(6)	$7p_{\frac{1}{2}}$–$7d_{\frac{3}{2}}$
3121.804(6)	3121.817		3.53×10^4	4.9	0.260(22)	$6d_{\frac{5}{2}}$–$5f_{\frac{7}{2}}$
3171.694(3)	3171.705		2.39×10^4	16.	0.123(8)	$6d_{\frac{3}{2}}$–$5f_{\frac{5}{2}}$
4186.610(5)	4186.614[a]	4186.62	5.04×10^5	5.8	0.186(16)	$6p_{\frac{3}{2}}$–$7s_{\frac{1}{2}}$
4363.021(6)	4363.016		4.32×10^4	6.9	0.103(20)	$7p_{\frac{3}{2}}$–$8d_{\frac{3}{2}}$
4382.191(3)	4382.197		4.57×10^5	12.	0.137(8)	$7p_{\frac{3}{2}}$–$8d_{\frac{5}{2}}$
4474.490(4)	4474.496		2.03×10^5	17.	0.124(11)	$7p_{\frac{1}{2}}$–$8d_{\frac{3}{2}}$
4484.795(5)	4484.882[a]	4484.88	2.94×10^5	3.3	0.113(18)	$6p_{\frac{1}{2}}$–$7s_{\frac{1}{2}}$
4484.938(7)			3.61×10^5	3.6	0.130(29)	
4486.227(9)	4486.221		4.45×10^5	3.1	0.241(35)	$6d_{\frac{5}{2}}$–$6f_{\frac{7}{2}}$
4536.097(3)	4536.095		3.18×10^5	20.	0.124(8)	$6d_{\frac{3}{2}}$–$6f_{\frac{5}{2}}$
4717.207(5)			1.86×10^5	8.7	0.157(17)	$4f$–$7g$
6792.022(4)	6792.083	6792.05	2.13×10^6	19.	0.227(12)	$5d_{\frac{5}{2}}$–$4f_{\frac{7}{2}}$
6815.400(6)	6815.389	6815.39	1.56×10^6	30.	0.136(8)	$5d_{\frac{3}{2}}$–$4f_{\frac{5}{2}}$

This theory has already been shown to be efficient in calculating the first-[45] and second-order[46,47] matrix elements in both atoms and molecules. To demonstrate that QDT calculations of the dipole transition matrix elements are sufficient for our line identification, we compared some QDT-calculated In oscillator strengths with experimental and theoretical data available in the literature.

In Table 3, we compare the QDT-calculated f-values with the results reported in other works and with those listed in the NIST database.[48] For the majority of the transitions, there is a satisfactory agreement between our QDT calculations and the experimental results obtained using the hook method [21,49] and using all-order relativistic many-body perturbation theory calculations.[50] For a few transitions, there are some discrepancies; for instance, Safronova *et al.* [50] reports the $\frac{5}{2}$–$\frac{5}{2}$ transition to be the strongest in the $4f$–$8d$ multiplet, which is most likely a misprint because general rules suggest that such a transition should be the weakest in the multiplet. However, the QDT calculations themselves are not our main aim in this work; we used these calculations in analyzing the relative intensities of the observed IR transitions. For calculating the matrix elements of the transitions involving g and h states, we use the energy levels values presented in Table 2.

Some difficulties arise in identifying the pair of lines at 2559.586 and 2559.638 cm^{-1}. According to the Rydberg formula and QDT calculations of line strengths, the $4f_{\frac{5}{2}}$–$5g_{\frac{7}{2}}$ and $4f_{\frac{7}{2}}$–$5g_{\frac{9}{2}}$ doublet should be the most prominent line near 2560 cm^{-1}. However, the observed doublet can also be due to the hyperfine structure of the $7s_{\frac{1}{2}}$–$7p_{\frac{1}{2}}$ line, whose center of gravity at 2559.584 cm^{-1} was reported by George *et al.* [19]. We are only able to resolve a two-peak hyperfine pattern of this line (as well as that of the $7s_{\frac{1}{2}}$–$7p_{\frac{3}{2}}$ line). From our experiment, the $7s_{\frac{1}{2}}$–$7p_{\frac{1}{2}}$ line has an intensity that is approximately 4.5 times greater (summed for the both peaks) than that of the $7s_{\frac{1}{2}}$–$7p_{\frac{3}{2}}$ line, as shown in Figure 4(b). However, in a non-relativistic approximation, the intensity of the $7s_{\frac{1}{2}}$–$7p_{\frac{3}{2}}$ line must be two times stronger.

We hypothesize that such a mismatch in the intensity distribution can be explained by the blending of the 2559.6 cm^{-1} line with a strong $4f$–$5g$ line whose fine-splitting pattern is not distinguishable from the hyperfine pattern of the $7s_{\frac{1}{2}}$–$7p_{\frac{1}{2}}$ line. Indeed, the oscillator strength of the $4f$–$5g$ line is by one order of magnitude higher than that of the $7s_{\frac{1}{2}}$–$7p_{\frac{1}{2}}$ line. Therefore, the mixture of a strong $4f$–$5g$ line breaks the non-relativistic ratio (1:2) of the intensities of the $7s_{\frac{1}{2}}$–$7p_{\frac{1}{2}}$ and $7s_{\frac{1}{2}}$–$7p_{\frac{3}{2}}$ lines. Futher evidence for the above observation comes after extraction of the $5g$ level from the measured $5g$–$7h$ line at 2161.471 cm^{-1}. Such an extraction can be performed by combining subsequently measured wavenumbers of the $6g$–$7h$ and $5f$–$6g$ transitions

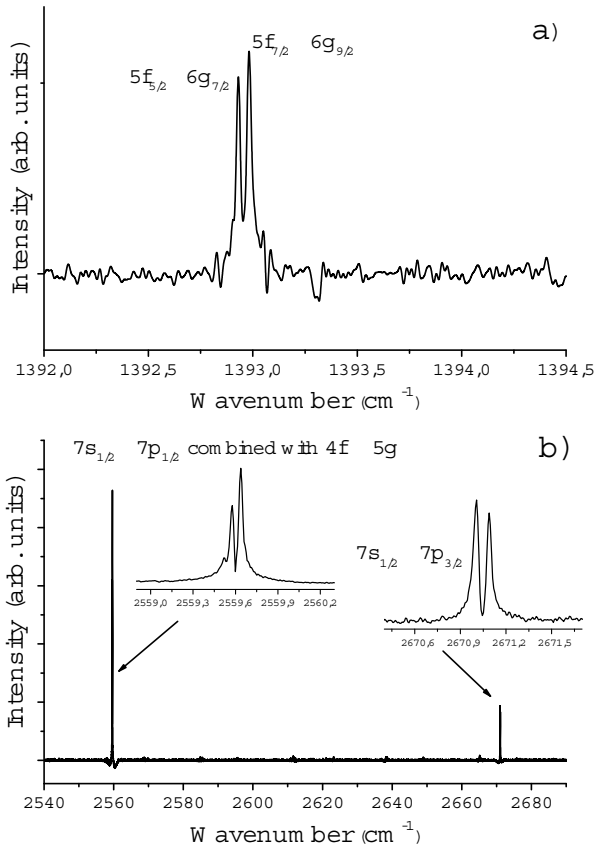

Fig. 4 Some parts of an emission spectra from a In I ablation plasma: a) newly observed multiplet lines $5f_{\frac{5}{2}}$–$6g_{\frac{7}{2}}$ and $5f_{\frac{7}{2}}$–$6g_{\frac{9}{2}}$; b) $7s$–$7p$ doublet with hyperfine structures shown in the insets. Note that the hyperfine structure of the $7s_{\frac{1}{2}}$–$7p_{\frac{1}{2}}$ line is combined with the fine structure of the $4f$–$5g$ line (see text).

with the known [19] energy value of the $5f$ level. Such a procedure gives $E_{5g} = 42267.182(22)$ cm^{-1}, which coincides within the uncertainty range with the $E_{5g} = 42267.175(21)$ cm^{-1} extracted from the 2559.586 and 2559.638 cm^{-1} lines based on the known [19] energy of the $4f$ level.

Table 2 presents the energy values, E_k, of the levels involved in the corresponding transitions, which were extracted from the measured ν_{ki} values from Table 1. The procedure of this refinement is briefly described in earlier papers.[33,34,36] The energies of the ng-levels ($n = 5, 6, 7$) and nh-levels ($n = 6, 7$) were not known before and are measured for the first time in the present work. Unfortunately, we were not able to resolve the fine-structure splitting of the f-levels. Within the uncertainties, our energies of the $nf_{\frac{5}{2}}$ and $nf_{\frac{5}{2}}$ levels ($n = 5, 6, 7$) do not differ, although the fine splitting of the $5f$–$6g$ line is clearly observed in Figure 4(a). We note that our energies of $E_{nf_{\frac{5}{2}}}$ and $E_{nf_{\frac{5}{2}}}$ that are listed in Table 2, coincide (within

the uncertainty range) with the corresponding values reported by [18] and are slightly closer to more recent results. [19]

Table 2 Energies of In I levels extracted from the measured spectra

Level	Energy (cm^{-1})	
	This work	Other sources
$7h$	44428.653(22)	
$7g$	44424.807(21)	
$7f$	44406.254(23)	44406.31(2),[18] 44406.23[19]
$6h$	43619.102(22)	
$6g$	43613.223(21)	
$6f_{\frac{7}{2}}$	43584.691(22)	43584.66(2),[18] 43584.681[19]
$6f_{\frac{5}{2}}$	43584.673(20)	43584.66(2),[18] 43584.681[19]
$5g$	42267.182(22)	
$5f_{\frac{7}{2}}$	42220.268(21)	42220.25(2),[18] 42220.281[19]
$5f_{\frac{5}{2}}$	42220.270(20)	42220.25(2),[18] 42220.281[19]
$4f_{\frac{7}{2}}$	39707.601(20)	39707.59(2),[18] 39707.622[19]
$4f_{\frac{5}{2}}$	39707.630(20)	39707.59(2),[18] 39707.161[19]

A large (beyond the uncertainty range) discrepancy in the $4f_{\frac{5}{2}}$ level energy is due, in our opinion, to a misprint in George *et al.* [19]. The only transition they were able to use for the extraction of $E_{4f_{\frac{5}{2}}}$ is their $5d_{\frac{3}{2}}$–$4f_{\frac{5}{2}}$ line at 6815.389 cm^{-1}. With their value of $E_{5d_{\frac{3}{2}}} = 32892.230$ cm^{-1}, a simple addition gives $E_{4f_{\frac{5}{2}}} = 32892.230 + 6815.389 = 39707.619$ cm^{-1} which agrees with our value of 39707.630(20) cm^{-1} (within the uncertainty range).

Transition $i \leftarrow k$	Lower level (cm^{-1})	Upper level (cm^{-1})	ν (cm^{-1})	$f_{ik} \times 100$ This work	$f_{ik} \times 100$ Other works
		$ns^2S - np^2P$			
$8s_{\frac{1}{2}}$–$8p_{\frac{1}{2}}$	40636.996 [19]	41827.167 [19]	1190.171	71.2	70.4 [50]
$8s_{\frac{1}{2}}$–$8p_{\frac{3}{2}}$	40636.996 [19]	41881.457 [19]	1244.461	142	140 [50]
$7s_{\frac{1}{2}}$–$7p_{\frac{1}{2}}$	36301.864 [19]	38861.448 [19]	2559.584	56.4	56.2 [50]
$7s_{\frac{1}{2}}$–$7p_{\frac{3}{2}}$	36301.864 [19]	38972.911 [19]	2671.047	113	112 [50]
$7s_{\frac{1}{2}}$–$8p_{\frac{1}{2}}$	36301.864 [19]	41827.167 [19]	5525.303	1.93	1.97 [50]
$7s_{\frac{1}{2}}$–$8p_{\frac{3}{2}}$	36301.864 [19]	41881.457 [19]	5579.593	4.94	5.04 [50]
$6s_{\frac{1}{2}}$–$6p_{\frac{1}{2}}$	24372.956 [19]	31816.982 [19]	7444.026	39.3	40.2 [50]
$6s_{\frac{1}{2}}$–$6p_{\frac{3}{2}}$	24372.956 [19]	32115.251 [19]	7742.295	79.5	81.3 [50]
$6s_{\frac{1}{2}}$–$7p_{\frac{1}{2}}$	24372.956 [19]	38861.448 [19]	14488.492	1.12	1.03 [50]
$6s_{\frac{1}{2}}$–$7p_{\frac{3}{2}}$	24372.956 [19]	38972.911 [19]	14599.955	3.01	2.84 [50]
$6s_{\frac{1}{2}}$–$8p_{\frac{1}{2}}$	24372.956 [19]	41827.167 [19]	17454.211	0.246	0.206 [50]
$6s_{\frac{1}{2}}$–$8p_{\frac{3}{2}}$	24372.956 [19]	41881.457 [19]	17508.501	0.731	0.642 [50]
		$np^2P - ns^2S$			
$7p_{\frac{3}{2}}$–$8s_{\frac{1}{2}}$	38972.911 [19]	40636.996 [19]	1664.085	41.1	42.0 [50]
$7p_{\frac{1}{2}}$–$8s_{\frac{1}{2}}$	38861.448 [19]	40636.996 [19]	1775.548	39.7	40.6 [50]
$6p_{\frac{3}{2}}$–$7s_{\frac{1}{2}}$	32115.251 [19]	36301.864 [19]	4186.613	26.2	27.9 [50]
$6p_{\frac{1}{2}}$–$7s_{\frac{1}{2}}$	31816.982 [19]	36301.864 [19]	4484.882	25.0	26.6 [50]
$6p_{\frac{3}{2}}$–$8s_{\frac{1}{2}}$	32115.251 [19]	40636.996 [19]	8521.745	2.07	2.06 [50]
$6p_{\frac{1}{2}}$–$8s_{\frac{1}{2}}$	31816.982 [19]	40636.996 [19]	8820.014	2.20	2.22 [50]
$5p_{\frac{3}{2}}$–$6s_{\frac{1}{2}}$	2212.599 [48]	24372.956 [19]	22160.357	9.14	14.2; [50] 15.3(7); [49] 14. [48]
$5p_{\frac{1}{2}}$–$6s_{\frac{1}{2}}$	0.	24372.956 [19]	24372.956	8.05	13.3; [50] 14.1(6); [49] 13. [48]
$5p_{\frac{3}{2}}$–$7s_{\frac{1}{2}}$	2212.599 [48]	36301.864 [19]	34089.265	1.44	1.53; [50] 1.7; [21] 1.5 [48]
$5p_{\frac{1}{2}}$–$7s_{\frac{1}{2}}$	0.	36301.864 [19]	36301.864	1.38	1.60; [50] 1.7; [21] 1.5 [48]
$5p_{\frac{3}{2}}$–$8s_{\frac{1}{2}}$	2212.599 [48]	40636.996 [19]	38424.397	0.545	0.541; [50] 0.58 [21]
$5p_{\frac{3}{2}}$–$9s_{\frac{1}{2}}$	2212.599 [48]	42719.031 [19]	40506.432	0.270	0.28 [21]
$5p_{\frac{1}{2}}$–$8s_{\frac{1}{2}}$	0.	40636.996 [19]	40636.996	0.527	0.507; [50] 0.58 [21]
$5p_{\frac{3}{2}}$–$10s_{\frac{1}{2}}$	2212.599 [48]	43881.314 [19]	41668.715	0.155	0.16 [21]
$5p_{\frac{3}{2}}$–$11s_{\frac{1}{2}}$	2212.599 [48]	44595.86 [48]	42383.261	0.0972	0.09 [21]
$5p_{\frac{1}{2}}$–$9s_{\frac{1}{2}}$	0.	42719.031 [19]	42719.031	0.262	0.29 [21]
$5p_{\frac{3}{2}}$–$12s_{\frac{1}{2}}$	2212.599 [48]	45067.19 [48]	42854.591	0.0651	0.07 [21]
$5p_{\frac{3}{2}}$–$13s_{\frac{1}{2}}$	2212.599 [48]	45394.13 [48]	43181.531	0.0458	0.04 [21]
$5p_{\frac{3}{2}}$–$14s_{\frac{1}{2}}$	2212.599 [48]	45630.44 [48]	43417.841	0.0335	0.04 [21]
$5p_{\frac{3}{2}}$–$15s_{\frac{1}{2}}$	2212.599 [48]	45806.88 [48]	43594.281	0.0252	0.03 [21]
		$np^2P - nd^2D$			
$6p_{\frac{3}{2}}$–$5d_{\frac{3}{2}}$	32115.251 [19]	32892.23 [19]	776.979	1.17	1.80 [50]
$6p_{\frac{3}{2}}$–$5d_{\frac{5}{2}}$	32115.251 [19]	32915.539 [19]	800.288	10.9	16.6 [50]
$6p_{\frac{1}{2}}$–$5d_{\frac{3}{2}}$	31816.982 [19]	32892.23 [19]	1075.248	16.3	22.5 [50]
$8p_{\frac{3}{2}}$–$8d_{\frac{5}{2}}$	41881.457 [19]	43335.108 [19]	1453.651	70.5	44.4 [50]

Table 3 QDT-calculated (this work) oscillator strengths ($f_{ik} \times 100$) of In I atom compared with other works. The Ritz wavenumbers ν are calculated using the energy level values from the cited references or from Table 2 (given witout references)

Table 3 – continued from previous page

Transition $i \leftarrow k$	Lower level (cm^{-1})	Upper level (cm^{-1})	ν (cm^{-1})	$f_{ik} \times 100$ This work	$f_{ik} \times 100$ Other works
$8p_{\frac{3}{2}}$–$8d_{\frac{3}{2}}$	41881.457 [19]	43335.937 [19]	1454.48	7.81	5.05 [50]
$8p_{\frac{1}{2}}$–$8d_{\frac{3}{2}}$	41827.167 [19]	43335.937 [19]	1508.77	69.2	42.7 [50]
$7p_{\frac{3}{2}}$–$7d_{\frac{3}{2}}$	38972.911 [19]	41836.443 [19]	2863.532	6.36	4.72 [50]
$7p_{\frac{3}{2}}$–$7d_{\frac{5}{2}}$	38972.911 [19]	41861.978 [19]	2889.067	54.1	41.6 [50]
$7p_{\frac{1}{2}}$–$7d_{\frac{3}{2}}$	38861.448 [19]	41836.443 [19]	2974.995	56.3	40.5 [50]
$7p_{\frac{3}{2}}$–$8d_{\frac{5}{2}}$	38972.911 [19]	43335.108 [19]	4362.197	13.9	11.7 [50]
$7p_{\frac{3}{2}}$–$8d_{\frac{3}{2}}$	38972.911 [19]	43335.937 [19]	4363.026	1.55	1.31 [50]
$7p_{\frac{1}{2}}$–$8d_{\frac{3}{2}}$	38861.448 [19]	43335.937 [19]	4474.489	14.8	12.0 [50]
$6p_{\frac{3}{2}}$–$6d_{\frac{3}{2}}$	32115.251 [19]	39048.576 [19]	6933.325	5.14	4.56 [50]
$6p_{\frac{3}{2}}$–$6d_{\frac{5}{2}}$	32115.251 [19]	39098.464 [19]	6983.213	43.9	40.4 [50]
$6p_{\frac{1}{2}}$–$6d_{\frac{3}{2}}$	31816.982 [19]	39048.576 [19]	7231.594	45.8	40.2 [50]
$6p_{\frac{3}{2}}$–$7d_{\frac{3}{2}}$	32115.251 [19]	41836.443 [19]	9721.192	1.29	1.19 [50]
$6p_{\frac{3}{2}}$–$7d_{\frac{5}{2}}$	32115.251 [19]	41861.978 [19]	9746.727	11.4	10.6 [50]
$6p_{\frac{1}{2}}$–$7d_{\frac{3}{2}}$	31816.982 [19]	41836.443 [19]	10019.461	12.4	11.2 [50]
$6p_{\frac{3}{2}}$–$8d_{\frac{5}{2}}$	32115.251 [19]	43335.108 [19]	11219.857	4.60	4.58 [50]
$6p_{\frac{3}{2}}$–$8d_{\frac{3}{2}}$	32115.251 [19]	43335.937 [19]	11220.686	0.512	0.511 [50]
$6p_{\frac{1}{2}}$–$8d_{\frac{3}{2}}$	31816.982 [19]	43335.937 [19]	11518.955	5.09	4.92 [50]
$5p_{\frac{3}{2}}$–$5d_{\frac{3}{2}}$	2212.599 [48]	32892.23 [19]	30679.631	3.38	3.98; [50] 6.0; [21] 4.8 [48]
$5p_{\frac{3}{2}}$–$5d_{\frac{5}{2}}$	2212.599 [48]	32915.539 [19]	30702.94	30.2	35.3; [50] 37; [21] 31.0 [48]
$5p_{\frac{1}{2}}$–$5d_{\frac{3}{2}}$	0.	32892.23 [19]	32892.23	29.5	36.1; [50] 36; [21] 30.8 [48]
$5p_{\frac{3}{2}}$–$6d_{\frac{3}{2}}$	2212.599 [48]	39048.576 [19]	36835.977	0.789	0.771; [50] 0.6 [21]
$5p_{\frac{3}{2}}$–$6d_{\frac{5}{2}}$	2212.599 [48]	39098.464 [19]	36885.865	7.12	6.81; [50] 5.2; [21] 4.5 [48]
$5p_{\frac{1}{2}}$–$6d_{\frac{3}{2}}$	0.	39048.576 [19]	39048.576	7.25	7.24; [50] 4.5; [21] 3.9 [48]
$5p_{\frac{3}{2}}$–$7d_{\frac{3}{2}}$	2212.599 [48]	41836.443 [19]	39623.844	0.295	0.271; [50] 0.14 [21]
$5p_{\frac{3}{2}}$–$7d_{\frac{5}{2}}$	2212.599 [48]	41861.978 [19]	39649.379	2.71	2.38; [50] 0.89 [21]
$5p_{\frac{3}{2}}$–$8d_{\frac{5}{2}}$	2212.599 [48]	43335.108 [19]	41122.509	1.22	1.13; [50] 1.3 [21]
$5p_{\frac{3}{2}}$–$8d_{\frac{3}{2}}$	2212.599 [48]	43335.937 [19]	41123.338	0.135	0.129 [50]
$5p_{\frac{1}{2}}$–$7d_{\frac{3}{2}}$	0.	41836.443 [19]	41836.443	2.79	2.56; [50] 0.59 [21]
$5p_{\frac{1}{2}}$–$8d_{\frac{3}{2}}$	0.	43335.937 [19]	43335.937	1.31	1.22; [50] 0.03 [21]
		$nd^2D - np^2P$			
$6d_{\frac{3}{2}}$–$8p_{\frac{1}{2}}$	39048.576 [19]	41827.167 [19]	2778.591	2.87	4.10 [50]
$6d_{\frac{5}{2}}$–$8p_{\frac{3}{2}}$	39098.464 [19]	41881.457 [19]	2782.993	3.00	4.01 [50]
$6d_{\frac{3}{2}}$–$8p_{\frac{3}{2}}$	39048.576 [19]	41881.457 [19]	2832.881	0.431	0.644 [50]
$5d_{\frac{3}{2}}$–$7p_{\frac{1}{2}}$	32892.23 [19]	38861.448 [19]	5969.218	1.50	1.86 [50]
$5d_{\frac{5}{2}}$–$7p_{\frac{3}{2}}$	32915.539 [19]	38972.911 [19]	6057.372	1.42	1.80 [50]
$5d_{\frac{3}{2}}$–$7p_{\frac{3}{2}}$	32892.23 [19]	38972.911 [19]	6080.681	0.230	0.290 [50]
$5d_{\frac{3}{2}}$–$8p_{\frac{1}{2}}$	32892.23 [19]	41827.167 [19]	8934.937	0.236	0.321 [50]
$5d_{\frac{5}{2}}$–$8p_{\frac{3}{2}}$	32915.539 [19]	41881.457 [19]	8965.918	0.227	0.317 [50]
$5d_{\frac{3}{2}}$–$8p_{\frac{3}{2}}$	32892.23 [19]	41881.457 [19]	8989.227	0.0368	0.0509 [50]

Table 3 QDT-calculated (this work) oscillator strengths ($f_{ik} \times 100$) of In I atom compared with other works. The Ritz wavenumbers ν are calculated using the energy level values from the cited references or from Table 2 (given witout references)

Table 3 – continued from previous page

Transition $i \leftarrow k$	Lower level (cm^{-1})	Upper level (cm^{-1})	ν (cm^{-1})	$f_{ik} \times 100$	
				This work	Other works
		$nd^2D - nf^2F$			
$6d_{\frac{5}{2}}$–$4f_{\frac{7}{2}}$	39098.464 [19]	39707.601	609.137	27.7	16.4 [50]
$6d_{\frac{5}{2}}$–$4f_{\frac{5}{2}}$	39098.464 [19]	39707.63	609.166	1.39	0.819 [50]
$6d_{\frac{3}{2}}$–$4f_{\frac{5}{2}}$	39048.576 [19]	39707.63	659.054	31.6	17.7 [50]
$8d_{\frac{3}{2}}$–$7f_{\frac{5}{2}}$	43335.937 [19]	44406.23 [19]	1070.293	18.5	
$8d_{\frac{5}{2}}$–$7f_{\frac{7}{2}}$	43335.108 [19]	44406.23 [19]	1071.122	17.5	
$8d_{\frac{5}{2}}$–$7f_{\frac{5}{2}}$	43335.108 [19]	44406.23 [19]	1071.122	0.874	
$7d_{\frac{5}{2}}$–$6f_{\frac{7}{2}}$	41861.978 [19]	43584.681 [19]	1722.703	30.6	
$7d_{\frac{5}{2}}$–$6f_{\frac{5}{2}}$	41861.978 [19]	43584.681 [19]	1722.703	1.53	
$7d_{\frac{3}{2}}$–$6f_{\frac{5}{2}}$	41836.443 [19]	43584.681 [19]	1748.238	29.4	
$7d_{\frac{5}{2}}$–$7f_{\frac{7}{2}}$	41861.978 [19]	44406.23 [19]	2544.252	11.4	
$7d_{\frac{5}{2}}$–$7f_{\frac{5}{2}}$	41861.978 [19]	44406.23 [19]	2544.252	0.570	
$7d_{\frac{3}{2}}$–$7f_{\frac{5}{2}}$	41836.443 [19]	44406.23 [19]	2569.787	11.3	
$6d_{\frac{5}{2}}$–$5f_{\frac{7}{2}}$	39098.464 [19]	42220.281 [19]	3121.817	47.5	50.7 [50]
$6d_{\frac{5}{2}}$–$5f_{\frac{5}{2}}$	39098.464 [19]	42220.281 [19]	3121.817	2.38	2.54 [50]
$6d_{\frac{3}{2}}$–$5f_{\frac{5}{2}}$	39048.576 [19]	42220.281 [19]	3171.705	47.0	52.4 [50]
$6d_{\frac{5}{2}}$–$6f_{\frac{7}{2}}$	39098.464 [19]	43584.681 [19]	4486.217	14.8	
$6d_{\frac{5}{2}}$–$6f_{\frac{5}{2}}$	39098.464 [19]	43584.681 [19]	4486.217	0.738	
$6d_{\frac{3}{2}}$–$6f_{\frac{5}{2}}$	39048.576 [19]	43584.681 [19]	4536.105	15.0	
$6d_{\frac{5}{2}}$–$7f_{\frac{7}{2}}$	39098.464 [19]	44406.23 [19]	5307.766	6.71	
$6d_{\frac{5}{2}}$–$7f_{\frac{5}{2}}$	39098.464 [19]	44406.23 [19]	5307.766	0.335	
$6d_{\frac{3}{2}}$–$7f_{\frac{5}{2}}$	39048.576 [19]	44406.23 [19]	5357.654	6.92	
$5d_{\frac{5}{2}}$–$4f_{\frac{7}{2}}$	32915.539 [19]	39707.601	6792.062	82.9	71.3 [50]
$5d_{\frac{5}{2}}$–$4f_{\frac{5}{2}}$	32915.539 [19]	39707.63	6792.091	4.15	3.56 [50]
$5d_{\frac{3}{2}}$–$4f_{\frac{5}{2}}$	32892.23 [19]	39707.63	6815.4	86.7	74.3 [50]
$5d_{\frac{5}{2}}$–$5f_{\frac{7}{2}}$	32915.539 [19]	42220.281 [19]	9304.742	17.8	15.2 [50]
$5d_{\frac{5}{2}}$–$5f_{\frac{5}{2}}$	32915.539 [19]	42220.281 [19]	9304.742	0.892	0.759 [50]
$5d_{\frac{3}{2}}$–$5f_{\frac{5}{2}}$	32892.23 [19]	42220.281 [19]	9328.051	18.7	15.9 [50]
$5d_{\frac{5}{2}}$–$6f_{\frac{7}{2}}$	32915.539 [19]	43584.681 [19]	10669.142	7.14	
$5d_{\frac{5}{2}}$–$6f_{\frac{5}{2}}$	32915.539 [19]	43584.681 [19]	10669.142	0.357	
$5d_{\frac{3}{2}}$–$6f_{\frac{5}{2}}$	32892.23 [19]	43584.681 [19]	10692.451	7.51	
$5d_{\frac{5}{2}}$–$7f_{\frac{7}{2}}$	32915.539 [19]	44406.23 [19]	11490.691	3.67	
$5d_{\frac{5}{2}}$–$7f_{\frac{5}{2}}$	32915.539 [19]	44406.23 [19]	11490.691	0.183	
$5d_{\frac{3}{2}}$–$7f_{\frac{5}{2}}$	32892.23 [19]	44406.23 [19]	11514.	3.87	
		$nf^2F - nd^2D$			
$5f_{\frac{7}{2}}$–$8d_{\frac{5}{2}}$	42220.281 [19]	43335.108 [19]	1114.827	13.6	8.09 [50]
$5f_{\frac{5}{2}}$–$8d_{\frac{5}{2}}$	42220.281 [19]	43335.108 [19]	1114.827	0.907	0.539 [50]
$5f_{\frac{5}{2}}$–$8d_{\frac{3}{2}}$	42220.281 [19]	43335.937 [19]	1115.656	12.7	7.75 [50]
$4f_{\frac{5}{2}}$–$7d_{\frac{3}{2}}$	39707.63	41836.443 [19]	2128.813	4.92	3.28 [50]

Table 3 QDT-calculated (this work) oscillator strengths ($f_{ik} \times 100$) of In I atom compared with other works. The Ritz wavenumbers ν are calculated using the energy level values from the cited references or from Table 2 (given witout references)

Table 3 – continued from previous page

Transition $i \leftarrow k$	Lower level (cm^{-1})	Upper level (cm^{-1})	ν (cm^{-1})	$f_{ik} \times 100$ This work	$f_{ik} \times 100$ Other works
$4f_{\frac{5}{2}}$–$7d_{\frac{5}{2}}$	39707.63	41861.978 [19]	2154.348	0.326	0.228 [50]
$4f_{\frac{7}{2}}$–$7d_{\frac{5}{2}}$	39707.601	41861.978 [19]	2154.377	4.89	3.42 [50]
$4f_{\frac{5}{2}}$–$8d_{\frac{5}{2}}$	39707.63	43335.108 [19]	3627.478	0.0527	3.51 [50]
$4f_{\frac{7}{2}}$–$8d_{\frac{5}{2}}$	39707.601	43335.108 [19]	3627.507	0.790	0.526 [50]
$4f_{\frac{5}{2}}$–$8d_{\frac{3}{2}}$	39707.63	43335.937 [19]	3628.307	0.736	0.502 [50]
		$nf^2F - ng^2G$			
$6f_{\frac{7}{2}}$–$7g_{\frac{9}{2}}$	43584.681 [19]	44424.807	840.126	99.0	
$6f_{\frac{7}{2}}$–$7g_{\frac{7}{2}}$	43584.681 [19]	44424.807	840.126	2.83	
$6f_{\frac{5}{2}}$–$7g_{\frac{7}{2}}$	43584.681 [19]	44424.807	840.126	102	
$5f_{\frac{7}{2}}$–$6g_{\frac{9}{2}}$	42220.281 [19]	43613.223	1392.942	110	
$5f_{\frac{7}{2}}$–$6g_{\frac{7}{2}}$	42220.281 [19]	43613.223	1392.942	3.14	
$5f_{\frac{5}{2}}$–$6g_{\frac{7}{2}}$	42220.281 [19]	43613.223	1392.942	113	
$5f_{\frac{7}{2}}$–$7g_{\frac{9}{2}}$	42220.281 [19]	44424.807	2204.526	23.2	
$5f_{\frac{7}{2}}$–$7g_{\frac{7}{2}}$	42220.281 [19]	44424.807	2204.526	0.662	
$5f_{\frac{5}{2}}$–$7g_{\frac{7}{2}}$	42220.281 [19]	44424.807	2204.526	23.8	
$4f_{\frac{5}{2}}$–$5g_{\frac{7}{2}}$	39707.63	42267.182	2559.552	138	
$4f_{\frac{7}{2}}$–$5g_{\frac{9}{2}}$	39707.601	42267.182	2559.581	134	
$4f_{\frac{7}{2}}$–$5g_{\frac{7}{2}}$	39707.601	42267.182	2559.581	3.84	
$4f_{\frac{5}{2}}$–$6g_{\frac{7}{2}}$	39707.63	43613.223	3905.593	21.2	
$4f_{\frac{7}{2}}$–$6g_{\frac{9}{2}}$	39707.601	43613.223	3905.622	20.6	
$4f_{\frac{7}{2}}$–$6g_{\frac{7}{2}}$	39707.601	43613.223	3905.622	0.588	
$4f_{\frac{5}{2}}$–$7g_{\frac{7}{2}}$	39707.63	44424.807	4717.177	7.25	
$4f_{\frac{7}{2}}$–$7g_{\frac{9}{2}}$	39707.601	44424.807	4717.206	7.05	
$4f_{\frac{7}{2}}$–$7g_{\frac{7}{2}}$	39707.601	44424.807	4717.206	0.201	
		$ng^2G - nf^2F$			
$6g_{\frac{9}{2}}$–$7f_{\frac{7}{2}}$	43613.223	44406.23 [19]	793.007	2.84	
$6g_{\frac{7}{2}}$–$7f_{\frac{7}{2}}$	43613.223	44406.23 [19]	793.007	0.101	
$6g_{\frac{7}{2}}$–$7f_{\frac{5}{2}}$	43613.223	44406.23 [19]	793.007	2.74	
$5g_{\frac{9}{2}}$–$6f_{\frac{7}{2}}$	42267.182	43584.681 [19]	1317.499	1.10	
$5g_{\frac{7}{2}}$–$6f_{\frac{7}{2}}$	42267.182	43584.681 [19]	1317.499	0.0394	
$5g_{\frac{7}{2}}$–$6f_{\frac{5}{2}}$	42267.182	43584.681 [19]	1317.499	1.07	
$5g_{\frac{9}{2}}$–$7f_{\frac{7}{2}}$	42267.182	44406.23 [19]	2139.048	0.183	
$5g_{\frac{7}{2}}$–$7f_{\frac{7}{2}}$	42267.182	44406.23 [19]	2139.048	0.00655	
$5g_{\frac{7}{2}}$–$7f_{\frac{5}{2}}$	42267.182	44406.23 [19]	2139.048	0.177	
		$ng^2G - nh^2H$			
$6g_{\frac{9}{2}}$–$7h_{\frac{11}{2}}$	43613.223	44428.653	815.43	136	
$6g_{\frac{9}{2}}$–$7h_{\frac{9}{2}}$	43613.223	44428.653	815.43	2.52	
$6g_{\frac{7}{2}}$–$7h_{\frac{9}{2}}$	43613.223	44428.653	815.43	139	
$5g_{\frac{9}{2}}$–$6h_{\frac{11}{2}}$	42267.182	43619.102	1351.92	131	

Table 3 QDT-calculated (this work) oscillator strengths ($f_{ik} \times 100$) of In I atom compared with other works. The Ritz wavenumbers ν are calculated using the energy level values from the cited references or from Table 2 (given witout references)

Table 3 – continued from previous page

Transition $i \leftarrow k$	Lower level (cm^{-1})	Upper level (cm^{-1})	ν (cm^{-1})	$f_{ik} \times 100$	
				This work	Other works
$5g_{\frac{9}{2}}$–$6h_{\frac{9}{2}}$	42267.182	43619.102	1351.92	2.43	
$5g_{\frac{7}{2}}$–$6h_{\frac{9}{2}}$	42267.182	43619.102	1351.92	134	
$5g_{\frac{9}{2}}$–$7h_{\frac{11}{2}}$	42267.182	44428.653	2161.471	12.1	
$5g_{\frac{9}{2}}$–$7h_{\frac{9}{2}}$	42267.182	44428.653	2161.471	0.224	
$5g_{\frac{7}{2}}$–$7h_{\frac{9}{2}}$	42267.182	44428.653	2161.471	12.3	
		$nh^2H - ng^2G$			
$6h_{\frac{9}{2}}$–$7g_{\frac{9}{2}}$	43619.102	44424.807	805.705	0.00384	
$6h_{\frac{11}{2}}$–$7g_{\frac{9}{2}}$	43619.102	44424.807	805.705	0.173	
$6h_{\frac{9}{2}}$–$7g_{\frac{7}{2}}$	43619.102	44424.807	805.705	0.169	

Table 3 QDT-calculated (this work) oscillator strengths ($f_{ik} \times 100$) of In I atom compared with other works. The Ritz wavenumbers ν are calculated using the energy level values from the cited references or from Table 2 (given witout references)

4 Conclusion

In this study, time-resolved FTIR spectroscopy was applied to measure the spectra of indium atoms produced by the laser ablation of an indium metal target with a natural isotopic composition. We cover the previously uninvestigated range from 800 to 2500 cm^{-1} and report the wavenumbers and emission intensities of 34 spectral lines, from which 17 transitions were observed experimentally for the first time. The experiment spectral data were used for the refinement of 12 indium energy levels, 5 of which (ng ($n = 5, 6, 7$) and nh ($n = 6, 7$) states) were previously unknown. The line classification was performed using relative line strengths that were calculated using single-channel quantum defect theory; these calculations show agreement with the experimental and calculated data available in the literature. We provide the calculated oscillator strengths between the levels involved in the observed transitions.

5 Acknowledgments

This work was financially supported by the by the Ministry of Education, Youth and Sports of the Czech Republic (grant LD14115 within the framework of the COST TD 1104 Action and grant LG13029). V.Ch. and E.Z. also acknowledge a partial support by the Ministry of Education and Science of Russia: State Order Project No.3.1306.2014/K (atomic QDT calculations) and Project No.1122 (analysis of IR spectra)

References

1 B. Klöter, C. Weber, D. Haubrich, D. Meschede and H. Metcalf, *Phys. Rev. A*, 2008, **77**, 033402.
2 B. K. Sahoo, R. Pandey and B. P. Das, *Phys. Rev. A*, 2011, **84**, 030502.
3 M. Das, R. K. Chaudhuri, S. Chattopadhyay and U. S. Mahapatra, *J. Phys. B*, 2011, **44**, 065003.
4 B. K. Sahoo and B. P. Das, *Phys. Rev. A*, 2011, **84**, 012501.
5 G. Ranjit, N. A. Schine, A. T. Lorenzo, A. E. Schneider and P. K. Majumder, *Phys. Rev. A*, 2013, **87**, 032506.
6 M. S. Safronova, U. I. Safronova and S. G. Porsev, *Phys. Rev. A*, 2013, **87**, 032513.
7 W. F. Meggers and R. J. Murphy, *J. Res. Nat. Bur. Stand.*, 1952, **48**, 334–344.
8 C. E. Moore, *Atomic energy levels as derived from the analyses of optical spectra*, U.S. Government Printing Office, 1958, vol. 3.
9 J. P. Connerade and M. A. Baig, *J. Phys. B*, 1981, **14**, 29–38.
10 H. Karlsson and U. Litzén, *J. Phys. B*, 2001, **34**, 4475–4485.
11 H. E. Clearman, *J. Opt. Soc. Am.*, 1952, **42**, 373–376.
12 G. V. Marr and R. Heppinstall, *Proc. Phys. Soc. (London)*, 1966, **87**, 547.
13 N. Karamatskos, M. Müller, M. Schmidt and P. Zimmermann, *J. Phys. B*, 1984, **17**, L341.
14 W. R. S. Garton, *Proc. Phys. Soc. Sect. A*, 1954, **67**, 864–868.
15 B. E. Krylov and M. G. Kozlov, *Opt. Spectrosc. (USSR)*, 1979, **47**, 579–582.
16 M. A. Baig, I. Ahmed and J. P. Connerade, *J. Phys. B*, 1988, **21**, 35.
17 H. Maeda, U. Eichmann and W. Sandner, *Phys. Rev. A*, 1998, **57**, 3376–3380.
18 I. Johansson and U. Litzén, *Ark. Fys. (Stockholm)*, 1967, **34**, 573587.
19 S. George, G. Guppy and J. Verges, *J. Opt. Soc. Am. B*, 1990, **7**, 249–252.
20 W. R. S. Garton and K. Codling, *Proc. Phys. Soc. (London)*, 1961, **78**, 600–606.
21 N. P. Penkin and L. N. Shabanova, *Opt. Spectrosc. (USSR)*, 1965, **18**, 425–431.
22 M. Y. Mirza and W. W. Duley, *Proc. R. Soc. London, Ser. A*, 1978, **364**, 255–263.
23 J. H. M. Neijzen and A. Dönszelmann, *Physica B+C*, 1981, **106**, 271 – 286.
24 J. H. M. Neijzen and A. Dönszelmann, *Physica B+C*, 1981, **111**, 127 – 133.
25 J. H. M. Neijzen and A. Dönszelmann, *Physica B+C*, 1982, **114**, 241 – 250.
26 G. J. N. E. de Vlieger, H. Wijnen and A. Dönszelmann, *Physica B+C*, 1983, **121**, 241 – 249.
27 R. Menges, G. Huber, G. Ulm and T. Kühl, *Z. Phys. A*, 1985, **320**, 575–578.
28 A. K. Kasimov, A. T. Tursunov and O. Tukhlibaev, *Opt. Spectrosc. (USSR)*, 1998, **84**, 482486.
29 S. Civiš, M. Ferus, P. Kubelík, P. Jelínek, V. E. Chernov and M. Y. Knyazev, *J. Opt. Soc. Am. B*, 2012, **29**, 1112–1118.
30 Civiš, S., Ferus, M., Kubelík, P., Jelinek, P. and Chernov, V. E., *Astron. Astrophys.*, 2012, **541**, A125.
31 K. Kawaguchi, N. Sanechika, Y. Nishimura, R. Fujimori, T. N. Oka, Y. Hirahara, A. Jaman and S. Civiš, *Chem. Phys. Lett.*, 2008, **463**, 38–41.
32 S. Civiš, I. Matulková, J. Cihelka, K. Kawaguchi, V. E. Chernov and E. Y. Buslov, *Phys. Rev. A*, 2010, **81**, 012510.
33 S. Civiš, I. Matulková, J. Cihelka, P. Kubelík, K. Kawaguchi and V. E. Chernov, *Phys. Rev. A*, 2010, **82**, 022502.
34 Civiš, S., Ferus, M., Kubelík, P., Jelinek, P., Chernov, V. E. and Zanozina, E. M., *Astron. Astrophys.*, 2012, **542**, A35.
35 Civiš, S., Ferus, M., Kubelík, P., Chernov, V. E. and Zanozina, E. M., *Astron. Astrophys.*, 2012, **545**, A61.
36 S. Civiš, M. Ferus, P. Kubelík, V. E. Chernov and E. M. Zanozina, *J. Phys. B*, 2012, **45**, 175002.
37 S. Civiš, M. Ferus, V. E. Chernov, E. M. Zanozina and L. Juha, *J. Quant. Spectrosc. Radiat. Transfer*, 2013, **129**, 324332.
38 S. Civiš, M. Ferus, V. E. Chernov, E. M. Zanozina and L. Juha, *J. Quant. Spectrosc. Radiat. Transfer*, 2014, **134**, 64 – 73.
39 M. Ferus, P. Kubelík, K. Kawaguchi, K. Dryahina, P. Španěl and S. Civiš, *J. Phys. Chem. A*, 2011, **115**, 1885–1899.
40 M. J. Hollas, *Modern Spectroscopy*, John Wiley & Sons Ltd, 2004.
41 S. Civiš, J. Cihelka and I. Matulková, *Opto-Electronics Review*, 2010, **18**, 408–420.
42 G. Smith, R. Palmer, J. Chalmers and P. Griffiths, in *Handbook of vibrational spectroscopy*, J. Wiley, 2002, pp. 625–640.
43 K. Kawaguchi, Y. Hama and S. Nishida, *J. Mol. Spectrosc.*, 2005, **232**, 1–13.
44 C. Aragon and J. A. Aguilera, *Spectrochim. Acta, Part B*, 2008, **63**, 893–916.
45 P. G. Alcheev, V. E. Chernov and B. A. Zon, *J. Mol. Spectrosc.*, 2002, **211**, 71–81.
46 V. E. Chernov, D. L. Dorofeev, I. Y. Kretinin and B. A. Zon, *Phys. Rev. A*, 2005, **71**, 022505.
47 E. V. Akindinova, V. E. Chernov, I. Y. Kretinin and B. A. Zon, *Phys. Rev. A*, 2009, **79**, 032506.
48 Y. Ralchenko, A. Kramida, J. Reader and NIST ASD Team, *NIST Atomic Spectra Database (version 5.0.0)*, http://physics.nist.gov/asd.
49 N. P. Penkin and L. N. Shabanova, *Opt. Spectrosc. (USSR)*, 1967, **23**, 11–16.

50 U. I. Safronova, M. S. Safronova and M. G. Kozlov, *Phys. Rev. A*, 2007, **76**, 022501.